

Efficient 3-D Fundamental LOD-FDTD Method Incorporated with Memristor

Zaifeng YANG^{†a)}, Member and Eng Leong TAN[†], Nonmember

SUMMARY An efficient three-dimensional (3-D) fundamental locally one-dimensional finite-difference time-domain (FLOD-FDTD) method incorporated with memristor is presented. The FLOD-FDTD method achieves higher efficiency and simplicity with matrix-operator-free right-hand sides (RHS). The updating equations of memristor-incorporated FLOD-FDTD method are derived in detail. Numerical results are provided to show the trade-off between efficiency and accuracy.

key words: memristor, FDTD, LOD-FDTD, unconditionally stable, fundamental scheme

1. Introduction

The memristor characterized by a relationship between the electric charge and flux was predicted by Chua in 1971 [1]. It is called the forth lumped element in addition to resistor, capacitor and inductor, but it did not cause a sensation at that time until 2008. Strukov *et al.* in Hewlett-Packard (HP) lab successfully fabricated a memristor using a thin film of titanium dioxide and a coupled variable-resistor physical model is given to describe its characteristics [2]. Subsequently, analyses and applications of memristor have attracted global attention from various research areas such as reconfigurable electromagnetic switching devices [3], microwave circuits [4], etc. The analyses and simulations of microwave circuits incorporated with memristor are usually implemented with resort to its SPICE model [5]. Meanwhile, computational electromagnetic methods such as finite-difference time-domain (FDTD) method incorporated with resistor, capacitor and inductor have been derived and widely utilized in microwave circuit simulation [6]. Recently, FDTD methods incorporated with memristor have been proposed in [7], [8]. Different from the lumped elements including resistor, capacitor and inductor, the forth lumped element bears the attributes of memory. The memristance will change according to the varying charge and flux.

Additionally, the time step of FDTD method is constrained by the Courant-Friedrich-Lewy (CFL) condition for a stable simulation. To enhance the computational efficiency, unconditionally stable FDTD methods have been proposed by using a larger time step. For three-dimensional (3-D) FDTD simulation, alternating-direction-

implicit FDTD (ADI-FDTD) [9], [10] and locally one-dimensional FDTD (LOD-FDTD) [11], [12] are two main classes of unconditionally stable FDTD methods. LOD-FDTD method is more efficient than ADI-FDTD method, but ADI-FDTD method has a higher (second-order) accuracy in time. To further enhance the computational efficiency, fundamental schemes [13], [14] can be implemented for the above unconditionally stable FDTD methods with matrix-operator-free right-hand sides (RHS). The unconditionally stable FDTD methods incorporated with lumped elements/devices have been developed to simulate microwave circuits including resistors, capacitors, inductors [15], [16] and diodes [17]. Nevertheless, to the best knowledge of the authors, there is no unconditionally stable method derived for memristor so far.

In this paper, an efficient 3-D fundamental LOD-FDTD (FLOD-FDTD) method incorporated with memristor is proposed. The FLOD-FDTD method achieves higher efficiency and simplicity with matrix-operator-free RHS. In Sect. 2, the updating equations of the FLOD-FDTD method incorporated with memristor are derived. In Sect. 3, numerical results will be provided to show the trade-off between efficiency and accuracy.

2. Efficient FLOD-FDTD Method Incorporated with Memristor

2.1 Modeling of Memristor

According to the coupled variable-resistor model proposed in [2], as shown in Fig. 1, the memristor can be considered as a resistor whose resistance is varied by the dopant width w . d is the thickness of the thin semiconductor film. If an external bias voltage across the memristor is applied, the boundary between the doped and undoped regions will move due to the drift of charged dopants. When the dopant width w approaches the whole thickness d , which is almost fully doped, the memristance is R_{ON} . Similarly, when the dopant width w approaches zero, the memristor is fully undoped and the memristance is R_{OFF} . Therefore, the memristance

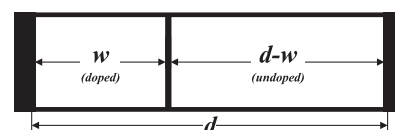


Fig. 1 The coupled variable-resistor model for memristor.

Manuscript received September 30, 2015.

Manuscript revised February 20, 2016.

[†]The authors are with the School of Electrical and Electronic Engineering, Nanyang Technological University, Singapore.

a) E-mail: Zyang007@e.ntu.edu.sg

DOI: 10.1587/transele.E99.C.788

is always varying within a bound from R_{ON} to R_{OFF} .

To show the state of the memristor, a variable x_{mem} with respect to time t is introduced to describe the extent of the doped width:

$$x_{mem}(t) = w(t)/d. \quad (1)$$

The relationship between the dopant state x_{mem} and the current $i(t)$ can be expressed as

$$\frac{dx_{mem}(t)}{dt} = \frac{1}{d} \frac{dw(t)}{dt} = \mu_v \frac{R_{ON}}{d^2} i(t) f(x_{mem}), \quad (2)$$

where μ_v is the average ion mobility and $f(x_{mem}) = 1 - (2x_{mem} - 1)^{2p}$. $f(x_{mem})$ is a non-linear window function [2], [8] that can make the state $x_{mem}(t)$ bounded within the interval $[0, 1]$, and p is the nonlinear exponent constant. As long as the state variable $x_{mem}(t)$ is calculated, the memristance $M_{mem}(t)$ with respect to time can be derived by

$$M_{mem}(t) = R_{ON}x_{mem}(t) + R_{OFF}[1 - x_{mem}(t)]. \quad (3)$$

2.2 LOD-FDTD Method with Memristor

The conventional 3-D LOD-FDTD method incorporated with memristor can be expressed in terms of two procedures as

$$(\mathbf{I} - \frac{\Delta t}{2}\mathbf{A})\mathbf{u}^{n+\frac{1}{2}} = (\mathbf{I} + \frac{\Delta t}{2}\mathbf{A})\mathbf{u}^n + \frac{\Delta t}{2}\mathbf{S}_{mem}^{n+\frac{1}{4}} \quad (4a)$$

$$(\mathbf{I} - \frac{\Delta t}{2}\mathbf{B})\mathbf{u}^{n+1} = (\mathbf{I} + \frac{\Delta t}{2}\mathbf{B})\mathbf{u}^{n+\frac{1}{2}} + \frac{\Delta t}{2}\mathbf{S}_{mem}^{n+\frac{3}{4}}, \quad (4b)$$

where

$$\mathbf{u} = [E_x, E_y, E_z, H_x, H_y, H_z]^T, \quad (5a)$$

$$\mathbf{S}_{mem} = \left[-\frac{1}{\varepsilon}J_{memx}, -\frac{1}{\varepsilon}J_{memy}, -\frac{1}{\varepsilon}J_{memz}, 0, 0, 0 \right]^T. \quad (5b)$$

Δx , Δy and Δz are the spatial steps along the x-,y- and z-directions, respectively; J_{memx} , J_{memy} and J_{memz} are the corresponding current density along the x-,y- and z-directions; \mathbf{A} and \mathbf{B} are the splitting matrices which are defined in [13].

The current density through a memristor in the first procedure from n to $n + \frac{1}{2}$ can be derived as (taking +z oriented memristor as an example)

$$\begin{aligned} J_{memz}|_{i+\frac{1}{2},j,k}^{n+\frac{1}{4}} &= \frac{V|_{i+\frac{1}{2},j,k}^{n+\frac{1}{4}}}{\Delta x \Delta y M_{memz}|_{i+\frac{1}{2},j,k}^{n+\frac{1}{4}}} \\ &= \frac{\Delta z (E_z|_{i+\frac{1}{2},j,k}^{n+\frac{1}{2}} + E_z|_{i+\frac{1}{2},j,k}^n)}{2\Delta x \Delta y M_{memz}|_{i+\frac{1}{2},j,k}^{n+\frac{1}{4}}}. \end{aligned} \quad (6)$$

where M_{memz} is the corresponding memristance along the z-direction. Similar equation can be written for the second procedure from $n + \frac{1}{2}$ to $n + 1$ with a change in the time index.

2.3 FLOD-FDTD Method with Memristor

To enhance the efficiency, the updating equations of FLOD-FDTD incorporated with memristor can be derived, free of matrix operator in RHS, by introducing an auxiliary variable:

$$\mathbf{v} = [e_x, e_y, e_z, h_x, h_y, h_z]^T \quad (7)$$

By manipulating (4) and (6), the FLOD-FDTD method incorporated with memristor can be written as:

$$(\frac{1}{2}\mathbf{I} - \frac{\Delta t}{4}\mathbf{A}_{mem})\mathbf{v}^{n+\frac{1}{2}} = \mathbf{u}^n \quad (8a)$$

$$\mathbf{u}^{n+\frac{1}{2}} = \mathbf{v}^{n+\frac{1}{2}} - \mathbf{u}^n \quad (8b)$$

$$(\frac{1}{2}\mathbf{I} - \frac{\Delta t}{4}\mathbf{B}_{mem})\mathbf{v}^{n+1} = \mathbf{u}^{n+\frac{1}{2}} \quad (8c)$$

$$\mathbf{u}^{n+1} = \mathbf{v}^{n+1} - \mathbf{u}^{n+\frac{1}{2}}. \quad (8d)$$

\mathbf{A}_{mem} and \mathbf{B}_{mem} are the modified splitting matrices for the memristor-incorporated FLOD-FDTD method:

$$\mathbf{A}_{mem} = \mathbf{A} - \frac{1}{2}\mathbf{diag}[\frac{d_{11}}{\varepsilon M_{memx}}, \frac{d_{22}}{\varepsilon M_{memy}}, \frac{d_{33}}{\varepsilon M_{memz}}, 0, 0, 0] \quad (9a)$$

$$\mathbf{B}_{mem} = \mathbf{B} - \frac{1}{2}\mathbf{diag}[\frac{d_{11}}{\varepsilon M_{memx}}, \frac{d_{22}}{\varepsilon M_{memy}}, \frac{d_{33}}{\varepsilon M_{memz}}, 0, 0, 0], \quad (9b)$$

where

$$d_{11} = \frac{\Delta x}{\Delta y \Delta z}, d_{22} = \frac{\Delta y}{\Delta x \Delta z}, d_{33} = \frac{\Delta z}{\Delta x \Delta y}. \quad (10)$$

It can be seen from (8a) and (8c) that their RHS are free of matrix operators. Thus, the efficiency is improved compared to the conventional LOD-FDTD with memristor.

2.4 Efficient Implementation

The efficient implementation of the 3-D FLOD-FDTD method incorporated with memristor in (8) can be exemplified by the E_z and H_z components in (11) (on next page). Equations (11a) and (11c) are the implicit update equations of e_z (auxiliary variable), while (11b) and (11d) are the explicit field components update equations of E_z and H_z for both procedures. After the implementation of the first procedure according to (11a) - (11b), the current through memristor can be calculated using Ampere's Law as

$$\begin{aligned} I_{memz}|_{i,j,k+\frac{1}{2}}^{n+\frac{1}{2}} &= (H_x|_{i,j-\frac{1}{2},k+\frac{1}{2}}^{n+\frac{1}{2}} - H_x|_{i,j+\frac{1}{2},k+\frac{1}{2}}^{n+\frac{1}{2}})\Delta x \\ &\quad + (H_y|_{i+\frac{1}{2},j,k+\frac{1}{2}}^{n+\frac{1}{2}} - H_y|_{i-\frac{1}{2},j,k+\frac{1}{2}}^{n+\frac{1}{2}})\Delta y. \end{aligned} \quad (12)$$

Since memristance will change according to the dopant state x_{mem} , x_{mem} will be updated for each sub time step. The

$$\left(\frac{1}{2} + \frac{\Delta t^2}{4\epsilon\mu\Delta x^2} + \frac{\Delta t d_{33}}{8\epsilon M_{memz}|_{i,j,k+\frac{1}{2}}^{n+1/4}}\right) e_z|_{i,j,k+\frac{1}{2}}^{n+\frac{1}{2}} - \frac{\Delta t^2}{8\epsilon\mu\Delta x^2} (e_z|_{i+1,j,k+\frac{1}{2}}^{n+\frac{1}{2}} + e_z|_{i-1,j,k+\frac{1}{2}}^{n+\frac{1}{2}}) = E_z|_{i,j,k+\frac{1}{2}}^n + \frac{\Delta t}{2\epsilon\Delta x} (H_y|_{i+\frac{1}{2},j,k+\frac{1}{2}}^n - H_y|_{i-\frac{1}{2},j,k+\frac{1}{2}}^n) \quad (11a)$$

$$E_z|_{i,j,k+\frac{1}{2}}^{n+\frac{1}{2}} = e_z|_{i,j,k+\frac{1}{2}}^{n+\frac{1}{2}} - E_z|_{i,j,k+\frac{1}{2}}^n, \quad H_z|_{i+\frac{1}{2},j+\frac{1}{2},k}^{n+\frac{1}{2}} = H_z|_{i+\frac{1}{2},j+\frac{1}{2},k}^n + \frac{\Delta t}{2\mu\Delta y} (e_x|_{i+\frac{1}{2},j+1,k}^{n+\frac{1}{2}} - e_x|_{i+\frac{1}{2},j,k}^{n+\frac{1}{2}}) \quad (11b)$$

$$\left(\frac{1}{2} + \frac{\Delta t^2}{4\epsilon\mu\Delta x^2} + \frac{\Delta t d_{33}}{8\epsilon M_{memz}|_{i,j,k+\frac{1}{2}}^{n+3/4}}\right) e_z|_{i,j,k+\frac{1}{2}}^{n+1} - \frac{\Delta t^2}{8\epsilon\mu\Delta y^2} (e_z|_{i,j+1,k+\frac{1}{2}}^{n+1} + e_z|_{i,j-1,k+\frac{1}{2}}^{n+1}) = E_z|_{i,j,k+\frac{1}{2}}^{n+\frac{1}{2}} + \frac{\Delta t}{2\epsilon\Delta y} (H_x|_{i,j+\frac{1}{2},k+\frac{1}{2}}^{n+\frac{1}{2}} - H_x|_{i+\frac{1}{2},j+\frac{1}{2},k-\frac{1}{2}}^{n+\frac{1}{2}}) \quad (11c)$$

$$E_z|_{i,j,k+\frac{1}{2}}^{n+1} = e_z|_{i,j,k+\frac{1}{2}}^{n+1} - E_z|_{i,j,k+\frac{1}{2}}^{n+\frac{1}{2}}, \quad H_z|_{i+\frac{1}{2},j+\frac{1}{2},k}^{n+1} = H_z|_{i+\frac{1}{2},j+\frac{1}{2},k}^{n+\frac{1}{2}} - \frac{\Delta t}{2\mu\Delta x} (e_y|_{i,j+\frac{1}{2},k+1}^{n+1} - e_y|_{i,j+\frac{1}{2},k}^{n+1}) \quad (11d)$$

dopant state of $+z$ oriented memristor $x_{memz}|_{i,j,k+\frac{1}{2}}^{n+\frac{3}{4}}$ can be derived from (2) and (12) as

$$x_{memz}|_{i,j,k+\frac{1}{2}}^{n+\frac{3}{4}} = x_{memz}|_{i,j,k+\frac{1}{2}}^{n+\frac{1}{4}} + \frac{\Delta t \mu_0 R_{ON}}{2d^2} f(x_{mem}) I_{memz}|_{i,j,k+\frac{1}{2}}^{n+\frac{1}{2}} \quad (13)$$

Subsequently, the update equation of the memristor $M_{memz}|_{i,j,k+\frac{1}{2}}^{n+\frac{3}{4}}$ can be written following (3) as

$$M_{memz}|_{i,j,k+\frac{1}{2}}^{n+\frac{3}{4}} = R_{ON} x_{memz}|_{i,j,k+\frac{1}{2}}^{n+\frac{3}{4}} + R_{OFF} [1 - x_{memz}|_{i,j,k+\frac{1}{2}}^{n+\frac{3}{4}}] \quad (14)$$

For implementation of the second procedure, similar update equation can be derived by adding $\frac{1}{2}$ to the time indices in (13) and (14). Note that the conventional FDTD coefficients for linear lumped elements are constant in time while the coefficients for the proposed FLOD-FDTD method with memristor will vary for different time step according to (14).

Because the memristor can be considered as a varying resistor within the interval $[R_{ON}, R_{OFF}]$, the lower bound of the doped state is 0 and the upper bound of the doped state is 1. The following bounding condition should be executed when (13) is updated:

$$x_{mem} = \begin{cases} 0, & x_{mem} < 0 \\ 1, & x_{mem} > 1. \end{cases} \quad (15)$$

Based on the above formulations, the time-stepping update equations for the proposed memristor-incorporated FLOD-FDTD method are summarized as

- Update the electromagnetic field components for the first procedure of FLOD-FDTD method from n to $n + \frac{1}{2}$ according to (8a) and (8b), e.g. (11a) and (11b).
- Calculate the current through memristor using (12), update the dopant state $x_{mem}^{n+\frac{3}{4}}$ using (13), and check the bounding condition of dopant state in (15).
- Update the memristance $M_{memz}|_{i,j,k+\frac{1}{2}}^{n+\frac{3}{4}}$ using (14).
- Update the electromagnetic field components for the

Table 1 Comparison of arithmetic operation counts in the RHS of one main iteration between 3-D LOD-FDTD and FLOD-FDTD.

Arithmetic operations (RHS)	LOD-FDTD with memristor	FLOD-FDTD with memristor
Implicit (M/D, A/S)	18, 24	6, 18
Explicit (M/D, A/S)	18, 36	18, 24
Total (M/D+A/S)	96	66

second procedure of FLOD-FDTD method from $n + \frac{1}{2}$ to $n + 1$ according to (8c) and (8d), e.g. (11c) and (11d).

- Calculate the current through memristor using (12), update the dopant state $x_{mem}^{n+1/4}$ using (13), and check the bounding condition of dopant state in (15).
- Update the memristance $M_{memz}|_{i,j,k+\frac{1}{2}}^{n+1/4}$ using (14). (The time indices in (12)-(14) should be changed accordingly for the second procedure.)

3. Comparison and Numerical Results

Table 1 shows the comparison of arithmetic operation counts in the RHS of one main iteration between 3-D LOD-FDTD and FLOD-FDTD. The number of multiplications/divisions (M/D) and additions/subtractions (A/S) are both counted in one main iteration with the assumption that all the multiplicative factors are pre-computed. It can be seen that the total arithmetic operation counts have been decreased for FLOD-FDTD method with memristor and the efficiency gain based on the total arithmetic operation counts in RHS is 1.45.

A numerical example is given to demonstrate the application of the proposed memristor-incorporated FLOD-FDTD method. A shielded microstrip line with a resistor and a memristor is simulated, where the geometry is shown in Fig. 2. Each cell is a cube with the side length of 1 mm. The computational domain is $100 \times 80 \times 30$. The resistor and memristor occupy one cell each and are connected to the microstrip line and ground by PEC wires. A current source is added at the center of the microstrip line: $J_z = 5000 \sin(2\pi ft) \text{A/m}^2$ with $f = 1 \text{GHz}$ flowing along z -axis from bottom to the microstrip line. The relative di-

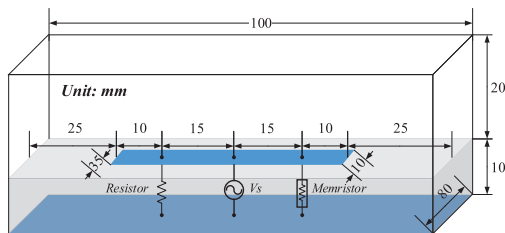


Fig. 2 Geometry of a shielded microstrip line with a resistor and a memristor.

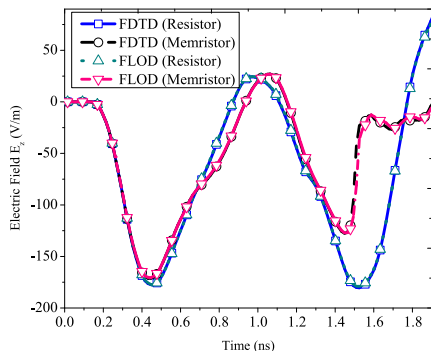


Fig. 3 Electric field E_z across the resistor and memristor using explicit FDTD method and FLOD-FDTD method when CFLN=1.

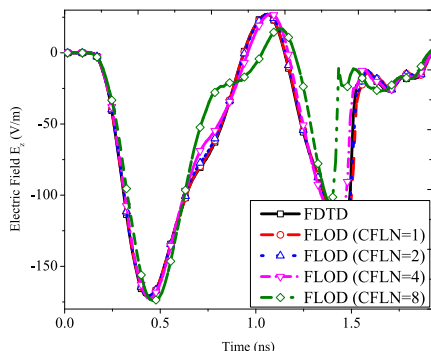


Fig. 4 Electric field E_z across the memristor using explicit FDTD method and FLOD-FDTD method when CFLN = 1, 2, 4 and 8.

electric constant of the microstrip substrate is 10 and the thickness is 10 mm. The thickness of the microstrip is set to 1 mm. The value of the resistor is $R = 5k\Omega$ and the initial value of the memristor is $5k\Omega$. The other parameters are $R_{ON} = 10\Omega$, $R_{OFF} = 10k\Omega$, $\mu_v = 1 \times 10^{-12}m/s$ and $d = 1 \times 10^{-12}m$. Figure 3 shows the electric field E_z across the resistor and memristor using explicit FDTD method and FLOD-FDTD method when CFLN=1, where $CFLN = \Delta t / \Delta t_{CFL}$. The time step is set to the CFL limit for the explicit FDTD. It can be observed that the electric field across the memristor deviates from the one of resistor. In addition, the results of FLOD-FDTD method when CFLN=1 agree well with the ones of explicit FDTD method.

Figure 4 shows the electric field E_z across the memristor using explicit FDTD method and FLOD-FDTD method when CFLN=1, 2, 4 and 8. It can be seen that the simu-

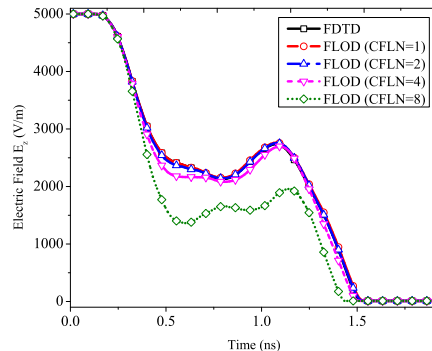


Fig. 5 Memristance across the memristor using explicit FDTD method and FLOD-FDTD method when CFLN = 1, 2, 4 and 8.

lated results of FLOD-FDTD method when CFLN=1, 2 and 4 agree well with the result of FDTD method, but the result of FLOD-FDTD method for CFLN=8 deviates from the other results to some extent. The larger time step will cause larger error of the update of memristance for each time step since the update of memristance is based on the calculated value from the previous time step.

Figure 5 shows the simulated memristances across the memristor using explicit FDTD method and FLOD-FDTD method when CFLN=1, 2, 4 and 8. Again, the simulated memristances of FLOD-FDTD method when CFLN=1, 2 and 4 agree well with the result of FDTD method, but the memristances of FLOD-FDTD method for CFLN=8 deviates from the other results to some degree. The trade-off between efficiency and accuracy has been illustrated here. We have quantified the errors and calculation time for different CFLNs for FLOD-FDTD method with memristor. The relative errors of FLOD-FDTD method with memristor compared with explicit FDTD method are 0.0071, 0.0393 and 0.2103 when CFLN is 2, 4 and 8, respectively. As the CFLN becomes larger, the operator splitting error [18] and the discretization error of the dopant states in (13) with larger time step would be the main reasons to cause more error. In addition, the calculated CPU time of the 3-D circuit in Fig. 2 from 0 to $1000\Delta t_{CFL}$ using the FLOD-FDTD method with memristor are 130.8 s and 65.3 s when CFLN are 4 and 8, while the explicit FDTD takes 147.8 s. Furthermore, through the simulation of the circuit in Fig. 2 for a long duration up to 100000 iterations (using CFLN=8), we have validated numerically the stability of our FLOD-FDTD method incorporated with memristor.

4. Conclusion

This paper has presented an efficient FLOD-FDTD method incorporated with memristor. The FLOD-FDTD achieves higher efficiency and simplicity with the removal of matrix operators in the RHS. The updating equations of the FLOD-FDTD method incorporating memristor has been derived. Numerical results have been provided to show the trade-off between efficiency and accuracy.

References

- [1] L.O. Chua, "Memristor-the missing circuit element," *IEEE Trans. Circuit Theory*, vol.18, no.5, pp.507–519, Sept. 1971.
 - [2] D.B. Strukov, G.S. Snider, D.R. Stewart, and S.R. Williams, "The missing memristor found," *Nature*, vol.453, pp.80–83, May 2008.
 - [3] G.B. Matthew and H.W. Douglas, "Passive switching of electromagnetic devices with memristors," *Appl. Phys. Lett.*, vol.96, no.7, pp.1625–1626, Feb. 2010.
 - [4] K.D. Xu, Y.H. Zhang, L. Wang, M.Q. Yuan, Y. Fan, W.T. Joines, and Q.H. Liu, "Two memristor SPICE models and their application in microwave devices," *IEEE Trans. Nanotechnol.*, vol.13, no.3, pp.607–616, March 2014.
 - [5] Z. Biolek, D. Biolek, and V. Biolkova, "SPICE model of memristor with nonlinear dopant drift," *Radioengineering*, vol.18, no.2, pp.210–214, June 2009.
 - [6] A. Taflove and S.C. Hagness, *Computational Electrodynamics: The Finite-Difference Time-Domain Method*, 3rd ed., Artech House, Boston, MA, 2005.
 - [7] Z. Yang and E.L. Tan, "Two finite-difference time-domain methods incorporated with memristor," *Progress In Electromagnetics Research M*, vol.42, pp.153–158, June 2015.
 - [8] M.D. Gregory and D.H. Werner, "Application of the memristor in reconfigurable electromagnetic devices," *IEEE Antennas Propag. Mag.*, vol.57, no.1, pp.239–248, June 2015.
 - [9] F. Zhen, Z. Chen, and J. Zhang, "Toward the Development of a Three-Dimensional Unconditionally Stable Finite-Difference time-domain method," *IEEE Trans. Microw. Theory Techn.*, vol.48, no.9, pp.1550–1558, Sept. 2000.
 - [10] T. Namiki, "3-D ADI-FDTD method-unconditionally stable time-domain algorithm for solving full vector Maxwell's equations," *IEEE Trans. Microw. Theory Techn.*, vol.48, no.10, pp.1743–1748, Oct. 2000.
 - [11] E.L. Tan, "Unconditionally stable LOD-FDTD method for 3-D Maxwell's equations," *IEEE Microw. Wireless Comp. Lett.*, vol.17, no.2, pp.85–87, Feb. 2007.
 - [12] J. Shibayama, R. Ando, J. Yamauchi, and H. Nakano, "A 3-D LOD-FDTD method for the wideband analysis of optical devices," *J. Lightw. Technol.*, vol.29, no.11, pp.1652–1658, June 2011.
 - [13] E.L. Tan, "Fundamental schemes for efficient unconditionally stable implicit finite-difference time-domain methods," *IEEE Trans. Antennas Propagat.*, vol.56, no.1, pp.170–177, Jan. 2008.
 - [14] J. Shibayama, T. Hirano, J. Yamauchi, and H. Nakano, "Efficient implementation of frequency-dependent 3D LOD-FDTD method using fundamental scheme," *Electronics Lett.*, vol.48, no.13, pp.774–775, June 2012.
 - [15] W. Fu and E.L. Tan, "Unconditionally stable ADI-FDTD method including passive lumped elements," *IEEE Trans. Electromagn. Compat.*, vol.48, no.4, pp.661–668, Nov. 2006.
 - [16] Z. Yang and E.L. Tan, "Efficient 3-D fundamental LOD-FDTD method with lumped elements," *2014 IEEE MTT-S Int. Microwave Symp. Dig.*, pp.1–3, June 2014.
 - [17] W. Yuan and E.-P. Li, "A stable algorithm for interfacing active and nonlinear devices with the ADI-FDTD method," *IEEE Microw. Wireless Comp. Lett.*, vol.15, no.12, pp.895–897, Dec. 2005.
 - [18] S.G. García, T.-W. Lee, and S.C. Hagness, "On the accuracy of the ADI-FDTD method," *IEEE Antennas Wireless Propag. Lett.*, vol.1, no.1, pp.31–34, Feb. 2002.
-